HIGH-ENERGY DIFFRACTION OF PARTICLES AND NUCLEI

László Jenkovszky [1]* ***and István Nagy*** [2]

[1] *Bogolyubov Institute for Theoretical Physics, National Academy of Sciences of Ukraine, Kiev, 03680 Ukraine*

[2] *Uzhgorod National University, Ukraine*

(Received October 28, 2011)

After a brief historical overview, we present recent results on high-energy diffraction, elastic and inelastic, with emphasis and comments on the recent experimental results from the Large Hadron Collider (LHC) at CERN.

PACS: 11.55.-m, 11.55.Jy, 12.40.Nn

1. INTRODUCTION

Modern high-energy diffraction of hadrons and nuclei, now known as the Glauber-Sitenko theory, to large extent was initiated by the seminal paper by A.I. Akhiezer and A.G. Sitenko [1]. The term, *diffraction* was introduced in nuclear high energy physics in the Fifties (for historical reviews and references see e.g. [2, 3]). The term is used in analogy with what was done for nearly two centuries in optics to describe the coherent phenomenon that occurs when a beam of light meets an obstacle or crosses a hole whose dimensions are comparable to its wavelength. Historically, the terminology comes from optics which, as a field, relies on approximations. Let us imagine a plane wave of wavelength λ which hits (perpendicularly, for simplicity) a screen with a hole of dimensions R and let us suppose that the wave number $k = \frac{2\pi}{\lambda}$ is sufficiently large that the short wavelength condition

$$kR >> 1 \tag{1.1}$$

is satisfied.

If Σ_0 describes the hole on the screen, according to the Huygens-Fresnel principle, each point becomes the center of a spherical wave whose envelope will give the deflected wave. Let Σ be the plane at a distance D where we imagine to collect the image (*i.e.* the detector plane). Because of the varying distances to the point and varying angles with respect to the original direction of the beam, the amplitudes and phases of the wavelets collected at each point will be different. As a consequence, cancelations and reinforcements can occur at different points giving rise to the phenomenon of diffraction. This propagation maps the value of this energy distribution T_0 on Σ_0) into its value T at the point $P(x, y, z)$ on the detector's plane. Mathematically, this is given by the Fresnel-Kirchhoff formula

$$T(x, y, z) = \frac{-i}{2\lambda}\frac{e^{ik_0 r_0}}{r_0}\int_\Sigma dS T_0[1 + \cos\theta]\frac{\exp i\vec{k}\cdot\vec{b}}{s}, \tag{1.2}$$

where $\vec{s}$ is the distance of the point P from Σ_0 and $\cos\theta$ is the inclination of this vector with respect to the normal to Σ_0.

The problem is greatly simplified when the detector is so distant that all rays from Σ_0 to the point $P(x, y, z)$ on Σ can be considered parallel. One talks of *Fraunhofer* or *Fresnel diffraction* according to whether the source is at a distance which can or cannot be considered infinitely large. For the case at hand, the large distance approximation will always be valid.

If the distance D satisfies the large distance condition

$$R/D << 1, \tag{1.3}$$

we may expand the exponential $\frac{e^{iks}}{s}$ in power series of ks. The following various cases can occur:

- *Fraunhofer diffraction* when

$$kR^2/D << 1; \tag{1.4a}$$

- *Fresnel diffraction* when

$$kR^2/D \approx 1; \tag{1.4b}$$

- *geometrical optics* when

$$kR^2/D >> 1. \tag{1.4c}$$

The consequence of all this is that the parameter kR^2/D is the one that dictates the optical regime.

In the Fraunhofer limit (1.4a) (which we shall be consistently assume), and turning to a terminology closer to that of particle physics by introducing the *impact parameter* $\vec{b}$, we shall rewrite Eq. (1.2) as

$$T(x, y, z) \approx \frac{k}{2\pi i}\frac{e^{ikr_0}}{r_0}\int_\Sigma d^2 b S(\vec{b}) e^{i\vec{q}\cdot\vec{b}} \tag{1.5}$$

*Corresponding author E-mail address: jenk@bipt.kiev.ua

where $\vec{q}$ is the two-dimensional momentum transfer

$$|\vec{q}| = k \sin\theta \tag{1.6}$$

and the scattering matrix S is expressed as

$$S(\vec{b}) \equiv 1 - \Gamma(\vec{b}) \tag{1.7}$$

in terms of the *profile function* of the target $\Gamma(\vec{b})$. Equivalently, inserting (1.7) into (1.5) one obtains the complete amplitude of which the term that contains 1 represents the unperturbed wave and the one that contains $\Gamma(\vec{b})$ is the diffracted wave.

The factor multiplying the outgoing spherical wave is the physically relevant quantity *i.e.* the scattering amplitude which we will write in the form

$$f(\vec{q}) = \frac{ik}{2\pi} \int d^2b\, \Gamma(\vec{b})\, e^{i\vec{q}\cdot\vec{b}}, \tag{1.8}$$

so that the scattering amplitude is given by the Fourier Transform of the profile function and, viceversa, we could also write

$$\Gamma(\vec{b}) = \frac{1}{2\pi ik} \int d^2q f(\vec{q}) e^{-i\vec{q}\cdot\vec{b}}. \tag{1.9}$$

If, now, the profile function $\Gamma(\vec{b})$ is spherically symmetric, Eq. (1.8) can be written as the Bessel Transform

$$f(\vec{q}) = ik \int_0^\infty bdb\Gamma(b) J_0(qb). \tag{1.10}$$

Finally, if the profile function is a disk of radius R, we obtain the so-called black disk form

$$f(\vec{q}) = ikR^2 \frac{J_1(qR)}{qR}. \tag{1.11}$$

The form (1.10) can be integrated explicitly for a number of cases but we shall not insist on these developments here.

Analyzing the optical limit and the diffraction of very high energy electromagnetic waves simulated by the collision of perfectly conducting spheres, one concludes that diffraction-like ideas applied to the realm of Maxwell equations describe electromagnetic waves correctly over at least 18 orders of magnitude from the Edison-Hertz to the HERA and LHC Colliders' wavelengths.

2. HIGH-ENERGY ELASTIC (DIFFRACTIVE) SCATTERING

The experimental data on proton-proton elastic and inelastic scattering emerging from the measurements at the LHC, call for an efficient model to fit the data and identify their diffractive (Pomeron) component. To this end, there is a need for a reasonably simple and feasible model of the scattering amplitude, yet satisfying the basic theoretical requirements such as analyticity, crossing and unitarity. In our opinion, the expected (dip-bump) structure in the differential cross section is most critical in discriminating models of high-energy diffraction, although other observables, such as the rate of the increase of the total cross sections, the ratio of the elastic to total cross section, detail concerning the shape of the elastic cross section, such as its "break" at small $|t|$ and flattening at large $|t|$ are important as well.

It was shown in paper [4] that, while the contribution from secondary Reggeons is negligible at the LHC, the inclusion of the Odderon (odd-C counterpart of the Pomeron) is mandatory, even for the description of pp scattering alone. To make our analyzis complete, we include in our fits $\bar{p}p$ data as well.

A supercritical ($\alpha_P(0) > 1$) Pomeron term, appended with non-leading (secondary) Reggeon contributions, with linear Regge trajectories describes elastic scattering data in a wide range of energies at small $-t$. Due to this simplicity it can be used also as a part of more complicated inelastic reactions, whenever Regge-factorization holds.

Any extension of this model should include:

- The dip-bump structure typical to high-energy diffractive processes;
- Non-linear Regge trajectories;
- Possible Odderon (odd-C asymptotic Regge exchange),and be
- Compatible with $s-$ and $t-$ channel unitarity;

The first attempt to describe high-energy diffraction, in particular the appearance of the characteristic dip-bump structure in the differential cross sections, was made by Chou and Yang [5], in which the distribution of matter in the nuclei was assumed to follow that of the electric charge (form factors). The original "geometrical" Chou and Young model [5] qualitatively reproduces the t dependence of the differential cross sections in elastic scattering, however it does not contain any energy dependence, subsequently introduced by means of Regge-pole models.

Following Ref. [4], we suggest a simple model that can be used as a handle in studying diffraction at the LHC. It combines the simplicity of the above models approach, and goes beyond their limitations. Being flexible, it can be modified according to the experimental needs or theoretical prejudice of its user and can be considered as the "minimal model" of high-energy scattering while its flexibility gives room for various generalizations/modifications or further developments (e.g. unitarization, inclusion of spin degrees of freedom etc.). We consider the spinless case of the invariant high-energy scattering amplitude, $A(s,t)$, where s and t are the usual Mandelstam variables. The basic assumptions of the model are:

1. The scattering amplitude is a sum of four terms, two asymptotic (Pomeron (P) and Odderon (O)) and two non-asymptotic ones or secondary Regge pole contributions.

2. We treat the Odderon, the C-odd counterpart of the Pomeron, on equal footing, differing by its $C-$ parity and the values of its parameters (to be fitted to the data).

3. The main subject is the Pomeron, and it is a double pole, or DP [3] lying on a nonlinear trajectory, whose intercept is slightly above one.

This choice is motivated by the unique properties of the DP: it produces logarithmically rising total cross sections at unit Pomeron intercept. By letting $\alpha_P(0) > 1$, we allow for a faster rise of the total cross section [1], although the intercept is about half that in the DP model since the double pole (or dipole) itself drives the rise in energy. Due to its geometric form (see below) the DP reproduces itself against unitarity (eikonal) corrections. As a consequence, these corrections are small, and one can use the model at the "Born level" without complicated (and ambiguous) unitarity (rescattering) corrections. DP combines the properties of Regge poles and of the geometric approach, initiated by Chou and Yang [5].

4. Regge trajectories are non-linear complex functions. In a limited range and with limited precision, they can be approximated by linear trajectories (which is a common practice, reasonable when non-linear effects can be neglected). This nonlinearity is manifest e.g. as the "break" i.e. a change the slope $\Delta B \approx 2$ GeV^2 around $t \approx -0.1$ GeV^2 and at large $|t|$, beyond the second maximum, $|t| > 2$ GeV^2, where the cross section flattens and the trajectories are expected to slowdown logarithmically.

In a simple mechanism of the diffractive dip-bump structure combining geometrical features and Regge behavior the dip is generated by the Pomeron contribution. The relevant Pomeron is a double pole arises from the interference between this dipole with a simple one, it is accompanied by. The dip-bump in the model shows correct dynamics, that is it develops from a shoulder, progressively deepening in the ISR energy region. As energy increases further, the dip is filled by the Odderon contribution. At low energies the contribution from non-leading, "secondary" Reggeons is also present.

The dipole Pomeron produces logarithmically rising total cross sections and nearly constant ratio of σ_{el}/σ_{tot} at unit Pomeron intercept, $\alpha_P(0) = 1$. While a mild, logarithmic increase of σ_{tot} does not contradict the data, the rise of the ratio σ_{el}/σ_{tot} beyond the SPS energies requires a supercritical DP intercept, $\alpha_P(0) = 1 + \delta$, where δ is a small parameter $\alpha_P(0) \approx 0.05$.

We use the normalization:

$$\frac{d\sigma}{dt} = \frac{\pi}{s^2}|A(s,t)|^2 \;\text{ and }\; \sigma_{tot} = \frac{4\pi}{s}\Im m A(s,t)\Big|_{t=0}. \tag{2.1}$$

The Pomeron term will be given below by Eq. (2.3) below. Secondary Reggeons are parametrized in a standard way [3], with linear Regge trajectories and exponential residua, where R denotes f or ω - the principal non-leading contributions to pp or $\bar{p}p$ scattering:

$$A_R(s,t) = a_R \mathrm{e}^{-i\pi\alpha_R(t)/2}\mathrm{e}^{b_R t}\Big(s/s_0\Big)^{\alpha_R(t)}, \tag{2.2}$$

with $\alpha_f(t) = 0.70 + 0.84t$ and $\alpha_\omega(t) = 0.43 + 0.93t$.

As argued above, the Pomeron is a dipole in the $j-$plane

$$A_P(s,t) = \frac{d}{d\alpha_P}\Big[\mathrm{e}^{-i\pi\alpha_P/2}G(\alpha_P)\Big(\frac{s}{s_0}\Big)^{\alpha_P}\Big] \tag{2.3}$$
$$= \mathrm{e}^{-i\pi\alpha_P(t)/2}\Big(\frac{s}{s_0}\Big)^{\alpha_P(t)}\Big[G'(\alpha_P) + \Big(L - \frac{i\pi}{2}\Big)G(\alpha_P)\Big].$$

Since the first term in squared brackets determines the shape of the cone, one fixes

$$G'(\alpha_P) = -a_P \mathrm{e}^{b_P[\alpha_P - 1]}, \tag{2.4}$$

where $G(\alpha_P)$ is recovered by integration, and, as a consequence, the Pomeron amplitude Eq. (2.3) can be rewritten in the following "geometrical" form (for the details of the calculations see [3] and references therein)

$$A_P(s,t) = i\frac{a_P\ s}{b_P\ s_0}\left\{r_1^2(s)\exp\left\{r_1^2(s)[\alpha_P - 1]\right\}\right.$$
$$\left. -\varepsilon_P r_2^2(s)\exp\left[r_2^2(s)[\alpha_P - 1]\right]\right\}, \tag{2.5}$$

where $r_1^2(s) = b_P + L - i\pi/2$, $r_2^2(s) = L - i\pi/2$, $L \equiv \ln(s/s_0)$.

The main features of the nonlinear trajectories are: 1) presence of a threshold singularity required by $t-$channel unitarity and responsible for the change of the slope in the exponential cone (the so-called "break") near $t = -0.1$ GeV^2, and 2) logarithmic asymptotic behavior providing for a power fall-off of the cross sections in the "hard" region. The combination of theses properties is however not unique, see [3]. An important property of the DP is the presence of absorptions, quantified by the value of the parameter ε_P in Eq. (2.5); this property, together with the non-linear nature of the trajectories, justifies the neglect of the rescattering corrections. The unknown Odderon contribution is assumed to be of the same form as that of the Pomeron, Eqs. (2.3) and (2.5), apart from different values of adjustable parameters (labeled by the subscript "O"):

$$A_O(s,t) = \frac{a_O\ s}{b_O\ s_0}[r_{1O}^2(s)\mathrm{e}^{r_{1O}^2(s)[\alpha_O - 1]}]. \tag{2.6}$$

The adjustable parameters are: δ_P, α_{iP}, a_P, b_P, ε_P for the Pomeron and δ_O, α_{iO}, a_O, b_O for the Odderon. Representative results are presented below in the figure.

[1] A supercritical Pomeron trajectory, $\alpha_P(0) > 1$ in the DP is required by the observed rise of the ratio σ_{el}/σ_{tot}, or, equivalently, departure form geometrical scaling.

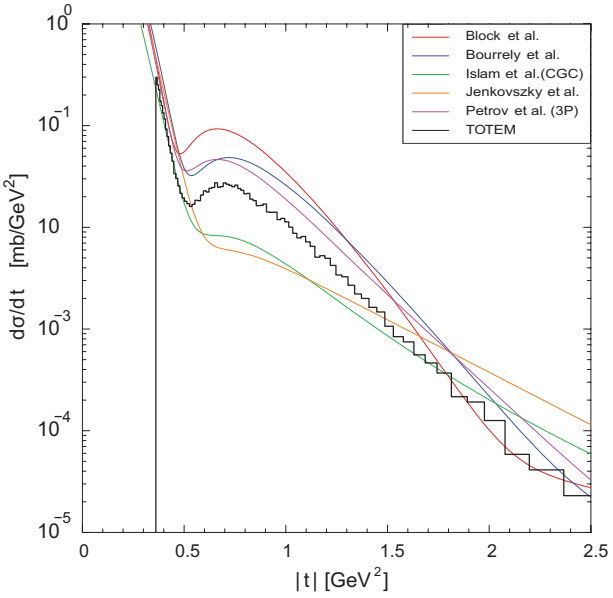

Elastic differential pp cross section as measured recently by the TOTEM Collaboration [6] at the LHC. Predictions by one of us (L.J. et al.) are also shown

The elastic cross section $\sigma_{el}(s)$ was calculated by integration

$$\sigma_{el} = \int_{t_{min}}^{t_{max}} (d\sigma/dt\, dt), \qquad (2.7)$$

where formally $t_{min} = -s/2$ and $t_{max} = t_{threshold}$. Since the integral is saturated basically by the first cone, we use $t_{max} = 0$ and $t_{min} = -25$ GeV^2 ($t_{min} = -3$ GeV^2 would do as well). Next we calculate $\sigma_{in}(s) = \sigma_{tot} - \sigma_{el}$.

It can be seen that starting from the Tevatron energy region, the relative contribution of the non-Pomeron terms to the total cross-section becomes smaller than the experimental uncertainty and hence at higher energies they may be completely neglected, irrespective of the model used. Such a discrimination (between Pomeron and non-Pomeron contributions) is more problematic in the non-forward direction, where the real and imaginary parts of various components of the scattering amplitude behave in a different way and the phase can not be controlled experimentally.

3. DIFFRACTION DISSOCIATION

The possible existence of a new class of processes, later named diffraction dissociation, for the first emphasized be A.I. Akhiezer and A.G. Sitenko [1]. The Experimentally, diffraction dissociation in proton-proton scattering was intensively studied in the '70-ies at the Fermilab and the CERN ISR.

Low-mass diffraction dissociation (DD) of protons, single

$$pp \to pX, \qquad (3.1)$$

and double, are among the priorities at the LHC.

While high-mass diffraction dissociation (DD) receives much attention, mainly due to its relatively easy theoretical treatment within the triple Reggeon formalism and successful reproduction of the data, this is not the case for low-masses, which are beyond the range of perturbative quantum chromodynamics (QCD). The forthcoming measurements at the LHC urge a relevant theoretical understanding and treatment of low mass DD, which essentially has both spectroscopic and dynamic aspects. The low-mass, M_X spectrum is rich of nucleon resonances. Their discrimination is a difficult experimental task, and theoretical predictions of the appearance of the resonances depending on s, t and M is also very difficult since, as mentioned, perturbative QCD, or asymptotic Regge pole formula are of no use here. With this paper we try to partially fill this gap, attacking the problem by means of a dual-Regge approach to the inelastic form factor (production amplitude) in which non-linear Regge trajectories play an essential role.

Diffraction, elastic and inelastic, in the LHC energy range is dominated by a single Pomeron exchange in the t channel, enabling the use of Regge factorization. Accordingly, the knowledge of two vertices and the Regge propagator is essential for the construction of the scattering amplitude. Relying on the known properties of the elastic proton-Pomeron-proton vertex and by adopting a simple supercritical Pomeron pole exchange (propagator) in the t channel, we concentrate on the construction of a proper inelastic proton-Pomeron-M_X vertex, the central object of our study. The solution of this problem, to large extent, became possible due to the similarity between the inelastic $\gamma^* p \to M_x$ and Pomeron+proton$\to M_x$ vertices.

The unknown inelastic form factOR, by the optical theorem, is related to the imaginary part of the forward $\gamma^*(P)-p$ scattering amplitude. we use a dual amplitude for this reaction, in its low-energy (here: missing mass), resonance region, dominated by the contribution of relevant direct-channel trajectories. The correct choice of these trajectories is a crucial point in our approach. In the case of $\gamma^* p$ scattering (e.g., JLab) these were the N^* and Δ trajectories. Here, instead, by quantum numbers, the relevant direct channel trajectory is that of the proton.

In principle, one could proceed by counting the resonances one-by-one; however, apart from the technical complexity of counting single resonances, there is also a conceptual one: Regge trajectories and, more generally, dual models comprise the dynamics in a complete and continuous way, thus opening the way to study and relate different reactions in any kinematical region. Examples are finite mass sum rules, contained in the present formalism automatically. One more important point: the advantage of using the dual-Regge model with non-linear Regge trajectory presented in this paper over a one-to-one account for the particular resonances is that it automatically takes care of the relative weight of each resonance, and extrapolates to higher masses, with a limited number of resonances on any trajectory.

Let us remind (see Sec. 2) the pp scattering amplitude

$$A(s,t) = -\beta^2[f^u(t)+f^d(t)]^2 \times \left(\frac{s}{s_0}\right)^{\alpha_P(t)-1} \frac{1+e^{-i\pi\alpha_P(t)}}{\sin\pi\alpha_P(t)}, \quad (3.2)$$

where $f^u(t)$ and $f^d(t)$ are the amplitudes for the emission of u and d valence quarks by the nucleon, β is the quark-Pomeron coupling, to be determined below; $\alpha_P(t)$ is a vacuum Regge trajectory. It is assumed that the Pomeron couples to the proton via quarks like a scalar photon. Thus, the unpolarized elastic pp differential cross section is

$$\frac{d\sigma}{dt} = \frac{[3\beta F^p(t)]^4}{4\pi\sin^2[\pi\alpha_P(t)/2]}(s/s_0)^{\alpha_P(t)-2}. \quad (3.3)$$

The norm β appearing in Eq. (3.3) was found from the forward elastic scattering, $d\sigma/dt \approx 80$ mb/GeV^2 at $\sqrt{s} = 23.6$ and 30.8 GeV, resulting, at unite Pomeron intercept, $\alpha_P(0) = 1$, in $\beta^4/(4\pi) \approx 1$ mb/GeV^2.

A dipole form can be used for the form factor

$$F^p(t) = \frac{4m^2-2.9t}{4m^2-t}\frac{1}{(1-t/0.71)^2}, \quad (3.4)$$

where m is the proton mass.

In single diffraction dissociation, Eq. (3.1), a system X with a missing mass M_X is produced at small $|t|$. At sufficiently large s/M_X^2, which is the case at the LHC, the process is dominated by a Pomeron exchange.

Similar to elastic scattering, Sec. 2, the double differential cross section for the reaction, by Regge factorization, can be written as

$$\frac{d^2\sigma}{dtdM_X^2} \sim \frac{9\beta^4[F^p(t)]^2}{4\pi\sin^2[\pi\alpha_P(t)/2]}(s/M_X^2)^{2\alpha_P(t)-2} \times\Big[\frac{W_2}{2m}\Big(1-M_X^2/s\Big) - mW_1(t+2m^2)/s^2\Big], \quad (3.5)$$

where W_i, $i=1,2$ are related to the structure functions of the nucleon and $W_2 \gg W_1$. For high M_X^2, the $W_{1,2}$ are Regge-behaved, while for small M_X^2 their behavior is dominated by nucleon resonances. Thus, the behavior of (3.5) in the low missing mass region to a large extent depends on the transition form factors or resonance structure functions. The knowledge of the inelastic form factors (or transition amplitudes) is crucial for the calculation of low-mass diffraction dissociation from Eq. (3.5).

At large s (the LHC energies), one can safely neglect terms M_X^2/s and $(t+2m^2)/s$ in Eq. (3.5). Furthermore, we have replaced the familiar form of the signature factor in the amplitude, $\frac{1+e^{-i\pi\alpha_P(t)}}{\sin\pi\alpha_P(t)}$ by a simple exponential one $e^{-i\pi\alpha_P(t)/2}$. For the proton elastic form factor $F^p(t)$, Eq. (3.4), we use a dipole form

$$F^p(t) = (1-t/0.71)^{-2}. \quad (3.6)$$

(note that here we neglect the first factor of Eq. (3.4) producing a break in the small $|t|$ behavior of the elastic differential cross section).

In the LHC energy region Eq. (3.5) simplifies to:

$$\frac{d^2\sigma}{dtdM_X^2} \approx \frac{9\beta^4[F^p(t)]^2}{4\pi}(s/M_X^2)^{2\alpha_P(t)-2}\frac{W_2}{2m}. \quad (3.7)$$

The one-by-one account for single resonances is a possible, although not efficient for the calculation of the SD cross section, to which, at low missing masses, a sequence of many resonances contribute. The definition and identification of these resonances is not unique; moreover with increasing masses (still within "low-mass diffraction"), they gradually disappear. Similar to the case of electroproduction, the (dis)appearance of resonances in the cross section depends on two variables, their mass and the virtuality or the "probe" (photon with Q^2 in electroproduction and Pomeron with t in SDD).

A way to account for many resonances is based on the ideas of duality with a limited number of resonances lying on non-linear Regge trajectories. The similarity between electroproduction of resonances (e.g. at JLab) and low-mass SDD is the key point of this approach [7]. The inelastic form factor (transition amplitude) is constructed by analogy with the nucleon resonances electroproduction amplitude. In both cases many resonances overlap and their appearance depends both on the reaction energy (here, missing mass) and virtuality of the incident probe (here the Pomoron's momentum transfer). This interplay makes the problem complicated and interesting.

For our purposes, i.e. for low-mass SDD, the direct-channel pole decomposition of the dual amplitude is relevant. Anticipating its application in SDD, we write it as [2]

$$A(M_X^2,t) = a\sum_{n=0,1,\dots}\frac{f(t)^{2(n+1)}}{2n+0.5-\alpha(M_X^2)},$$

where $\alpha(M_X^2)$ is a non-linear Regge trajectory in the Pomeron-proton system, t is the squared transfer momentum in the $Pp\to Pp$ reaction, and a is the normalization factor, which will be absorbed together with β in the overall normalization coefficient A_0 to be fitted to the data. We remind once again that here M_X^2 replaces s (the direct, Pp channel "energy").

The inelastic form form factor in diffraction dissociation is similar to that in γ^*p, up to the replacement of the photon by a Pomeron, whose parity is different from that of the photon. As a consequence, we have a single direct channel resonance trajectory, that of the proton, plus the exotic, nonresonance trajectory providing the background, dual to the Pomeron exchange in the cross channel.

Then we proceed:

$$W_2(M_X^2,t) = \frac{-t(1-x)}{4\pi\alpha_s(1+4m^2x^2/(-t))}\mathrm{Im}\,A(M_X^2,t),$$

[2] Note that resonances on the proton trajectory appear with spins $J = 1/2,\ 5/2,\ 9/2,\ 13/2$....

where x is the Bjorken variable, related to t and M_X^2 via $M_X^2 = m^2 - t(1-x)/x$. The imaginary part of the transition amplitude reads

$$\mathrm{Im}\, A(M_X^2, t) =$$

$$a \sum_{n=0,1,\ldots} \frac{[f(t)]^{2(n+1)} \mathrm{Im}\, \alpha(M_x^2)}{(2n + 0.5 - Re\, \alpha(M_X^2))^2 + (\mathrm{Im}\, \alpha(M_X^2))^2}.$$

Apart from the well established proton trajectory, with a sequence of four particles on it, there is a prominent resonance $I = 1/2, \;\; J = 1/2^+$ with mass 1440 MeV, known as the Roper resonance. It is wide, the width being nearly one quarter of its mass. The Roper resonance may appear on the daughter trajectory of N^* treated above, although its status is still disputable.

To calculate the integrated SDD we first take into account the contribution from the resonance region. This is done by integrating Eq. (3.6) in squared momentum transfer t from $-\infty$ to 0, and in the missing mass M_x over the resonance region, 2 GeV^2 $< M_x^2 <$ 8 GeV^2, where the contributions from the resonances, Eq. (3.6) dominate. We, thus, eliminate contributions from the region of the elastic peak, $M_X^2 <$ 2 GeV^2, that requires separate treatment, see [7], and the high missing mass Regge-behaved region. By duality, to avoid "double counting", the latter should be accounted for automatically, provided the resonance contribution is included properly.

Having fixed the parameters of the model, one can now scrutinize the SDD cross section in more details. First one calculates [7] from Eq. (3.6), double differential cross section as function of the missing mass for several fixed values of the momentum transfer t and two representative LHC energies, 7 and 14 TeV.

The elastic contribution, $pp \to pp$ is usually calculated and measured separately. There is no consistent theoretical prescription of any smooth transition from inelastic to elastic scattering, corresponding to the $x \to 1$ limit for the structure functions (see Ref. [7]).

The work of L.J. was supported by the program "Matter under Extreme Conditions" of the Department of Astronomy and Physics of the National Academy of Sciences of Ukraine.

References

1. A.I. Akhiezer and A.G. Sitenko. Diffractional Scattering of Fast Deutrons by Nuclei // *Phys. Rev.* 1957, v. 166, p. 1236.

2. V. Barone and E. Predazzi. *High-energy Particle Diffraction.* Springer-Verlag, 2002.

3. L. Jenkovszky. Phenomenology of Elastic Hadron Diffraction // *Fortschritte der Physik.* 1968, v. 34, p. 791; L. Jenkovszky. High-Energy Elastic Hadron Scattering // *Rivista Nuovo Cim.* 1987, v. 10, p. 1; A.N. Vall, L.L. Jenkovszky, and B.V. Struminsky. Hadrons' Structure and they High-Energy Interaction // *EChAYa (English translation: PEPAN).* 1988, v. 19, p. 180; L. Jenkovszky. Diffraction in Hadron-Hadron and Lepton-Hadron Processes at High Energies // *EChAYa (Engl. translation: PEPAN)*, 2003, v. 34, p. 1196; R. Fiore, L. Jenkovszky, R. Orava, E. Predazzi, A. Prokudin, and O. Selyugin. Forward Physics at the LHC: Elastic Scattering // *Int'l J. Mod. Phys.* 2009, v. A24, p. 2551; *arXiv*: 0812.0539 [hep-ph].

4. L.L. Jenkovszky, A.I. Lengyel, D. Lontkovskiy. The Pomeron and Odderon in elastic, inelastic and total cross sections at the LHC // *Int'l. J. Mod. Phys.* (in press).

5. T.T. Chou and C.N. Yang. A Geometrical Model of Strong Interaction // *Phys. Rev. Lett.* 1968, v. 20, p. 1615.

6. G. Antchev et al. [TOTEM Collaboration]. Proton-proton elastic scattering at the LHC energy at 7 TeV // *Europhys. Lett.* 2011, v. 95, 41001; *arXiv*: 1110.1385.

7. L.L. Jenkovszky, O. Kuprash, J. Lamsa, V. Magas, and R. Orava. Dual-Regge Approach to High-Energy // *Phys. Rev.* 2011, v. D83, 056014; L. Jenkovszky, O. Kuprash, V. Magas. Low-Mass Diffraction Dissociation // *Ukr. J. Phys.* 2011, v. 56, p. 738-743.

ДИФРАКЦИЯ АДРОНОВ И ЯДЕР ПРИ ВЫСОКИХ ЭНЕРГИЯХ

Ласло Енковский, Иштван Надь

После краткого исторического введения представлены новые результаты об упругой и неупругой дифракциях с учетом недавних экспериментальных результатов, полученных на Большом Адронном Коллайдере.

ДИФРАКЦІЯ АДРОНІВ ТА ЯДЕР ПРИ ВИСОКИХ ЕНЕРГІЯХ

Ласло Енковський, Іштван Надь

Після короткого історичного вступу представлено нові результати про пружню та непружню дифракції з врахуванням нещодавних експериментальних результатів з Великого Адронного Колайдера.